J Mater Sci (2009) 44:102–107
DOI 10.1007/s10853-008-3113-0

Compressive deformation behavior of ternary compound Cr_2AlC

Wubian Tian · ZhengMing Sun · Hitoshi Hashimoto · Yulei Du

Received: 15 August 2008 / Accepted: 10 November 2008 / Published online: 5 December 2008

Abstract The compressive properties of ternary compound Cr_2AlC at different temperatures and strain rates were studied. When tested at a strain rate of 5.6×10^{-4} s^{-1}, the compressive strength decreases continuously from 997 ± 29 MPa at room temperature to 523 ± 7 MPa at 900 °C. The ductile-to-brittle transition temperature is measured to be in the range of 700 to 800 °C. When tested in the strain rate range of 5.6×10^{-5} to 5.6×10^{-3} s^{-1}, Cr_2AlC fails in a brittle mode at room temperature, whereas the deformation mode changes from a brittle to a ductile as the strain rate is lower than 5.6×10^{-4} s^{-1} when compressed at 800 °C. The compressive strength increases slightly with increasing strain rate at room temperature and it is less dependent on strain rate when tested at 800 °C. The plastic deformation mechanism of Cr_2AlC was discussed in terms of dislocation-related activities, such as kink band formation, delamination, decohesion of grain boundary, and microcrack formation.

Introduction

In recent years, a series of ternary carbides and nitrides, abbreviated as $M_{n+1}AX_n$ (where $n = 1$–3, M is an early transition metal, A is an A group element, and X is C and/or N), have been studied extensively because of their good combination of various properties, such as high mechanical strength, good electrical and thermal conductivity as well as good chemical stability under oxidation and/or corrosion environments [1–4].

As a member of the M_2AX family, Cr_2AlC was reported by Jeitschko et al. in the 1960s [5]. Nearly 20 years later, Schuster et al. [6] synthesized the compound and identified its lattice parameters and phase relationship in the Cr–Al–C system. Recently, Schneider et al. [7] prepared Cr_2AlC film and studied its elastic properties [8]. Walter et al. [9, 10] fabricated and developed the application of Cr_2AlC film as protective coatings on steel. Lin et al. [11] reported the fabrication, transmission electron microscope characterization [12], and the oxidation behavior of bulk Cr_2AlC [13]. On the other hand, elastic properties of M_2AlC were studied by first principles calculation in recent years [14–18], in which Cr_2AlC was reported to possess high elastic stiffness, though the experimental modulus [8, 13, 19] is significantly lower.

Tian et al. [20] studied the isothermal oxidation behavior of Cr_2AlC ceramics in air at 1100 and 1250 °C for 20 h and found that Cr_2AlC shows good oxidation resistance at the testing temperatures. The electrical and thermal properties of Cr_2AlC at room and elevated temperatures were also reported [19]. Furthermore, its mechanical properties at room temperature such as hardness, elastic modulus, and damage tolerance as well as thermal shock properties were also investigated [21]. However, there is no further report on the mechanical properties, such as high temperature strength and deformation behavior, of Cr_2AlC as far as we know. As a potential candidate of high-temperature materials, the investigation of the mechanical properties at elevated temperature of this compound is a must before its practical application. In this article, therefore, we report the compressive behavior of Cr_2AlC at different temperatures and/or different strain rates.

W. B. Tian · Z. M. Sun (✉) · H. Hashimoto · Y. L. Du
Materials Research Institute for Sustainable Development, National Institute of Advanced Industrial Science and Technology (AIST), Nagoya 463-8560, Japan
e-mail: z.m.sun@aist.go.jp

W. B. Tian
e-mail: w.b.tian@aist.go.jp

Experimental procedure

The starting materials used in this study were chromium (ca. 10 μm, >98%), aluminum (ca. 10 μm, 99.9%), and graphite (ca. 5 μm, 99.7%) (all the materials purchased from Kojundo Chemical Lab., Japan). The powders were weighed according to the designed composition (molar ratio of Cr:Al:C = 2:1.1:1) that was usually used to synthesize Cr_2AlC [19, 20] and mixed by a Turbula shaker mixer for 24 h. The powder mixture was put into a graphite mold and sintered in vacuum using a pulse discharge sintering (PDS) equipment (PAS-V, Sodick Co. Ltd., Japan) at 1250 °C for 30 min with a heating rate of 50 °C/min and a pressure of 50 MPa.

The compressive specimens were cut by an electric discharge machine from the sintered bulk Cr_2AlC. Then, all the specimens were mechanically ground and polished to a dimension of 2.5 × 2.5 × 6 mm^3 with smooth surfaces for microscopic observation. The compressive tests were performed with an Instron 8562 universal testing machine at a strain rate (5.6×10^{-4} s^{-1}) between room temperature and 900 °C, and at different strain rates (5.6×10^{-5} to 5.6×10^{-3} s^{-1}) at room temperature and an elevated temperature of 800 °C, respectively. Three specimens were used for testing at each testing temperature or strain rate. Data were collected as engineering strain, and the recorded load–displacement data during testing were corrected by eliminating the system compliances which were experimentally determined at each individual testing condition (strain rate, temperature). The corrected load–displacement relationship of Cr_2AlC specimens was fairly close to its real value by examining the stress–strain relationship at the elastic part of deformation. For instance, the Young's modulus of the Cr_2AlC specimens measured from such determined stress–strain curve at room temperature at a strain rate of 5.6×10^{-4} s^{-1} is about 230 GPa, which is reasonably close to the experimental value of 278 GPa [19].

The density of sintered Cr_2AlC sample was measured by Archimedes principle. Phase content was determined by X-ray diffractometry (XRD) (X'pert, Philips, Netherlands) with Cu Kα radiation at 30 kV and 40 mA at a scanning speed of 0.02°/s. The sample was mechanically polished and etched in HF acid for 2 min before scanning electron microscope (SEM) observation. The observations on etched surfaces and fracture surfaces were performed under an SEM (FEI XL30S FEG, Netherlands) equipped with an energy-dispersive spectroscopy (EDS) system.

Results and discussion

Characterization

The XRD pattern of the sintered Cr_2AlC is shown in Fig. 1a, in which all the reflections can be indexed as Cr_2AlC according to JCPDS29-0017 and the peaks at 51.22, 63.06, and 67.01 degrees as the reflections of Cr_2AlC (105), (107), and (112) respectively as reported in ref. [11]. Measured density of the sample is 5.14 g/cm^3, which is 98% of the theoretical density. A typical backscattered SEM image of the etched surface of sintered Cr_2AlC sample is shown in Fig. 1b, in which the gray matrix phase corresponds to Cr_2AlC with a small amount of dark pores inside grains and some bright phases correspond to Cr_7C_3 that were usually found in the synthesized Cr_2AlC. Some dark gray grains that mainly distributed at tri-grain boundaries are identified to be Al_2O_3 according to EDS results (data not shown). This might be a result of the reaction between Al and the absorbed oxygen in starting powder. In addition, Cr_2AlC grains are mostly equiaxed and the average grain size is 6.4 ± 2.1 μm.

Compression at different temperatures and strain rates

The relationship between compressive stress and engineering strain in the temperature range of room temperature

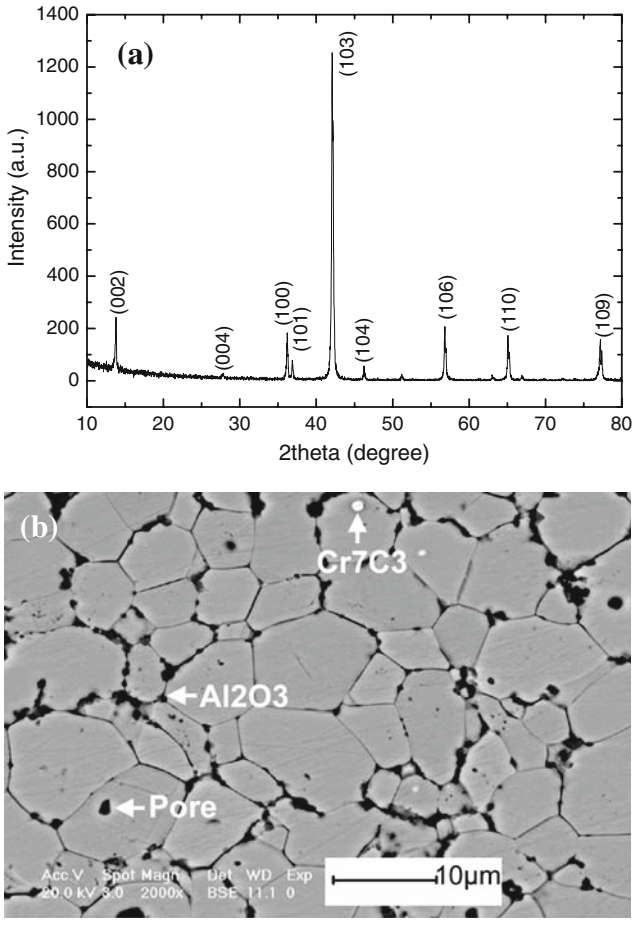

Fig. 1 **a** XRD pattern of Cr_2AlC sample sintered at 1250 °C for 30 min by PDS. **b** A typical backscattered SEM micrograph image on the surface of polished and etched sample

to 900 °C at a strain rate of 5.6×10^{-4} s^{-1} is shown in Fig. 2a (for clarity, curves are shifted). It is evident that the Cr_2AlC specimens fail abruptly in a brittle mode after the maximum compressive stress is reached when tested below 700 °C. However, an obviously plastic deformation region is observed on the stress–strain curves when tested at temperatures higher than 800 °C, and this region becomes broadened at 900 °C. In fact, the specimen tested at 900 °C does not break but is deformed to a spindle-like shape. Therefore, the ductile-to-brittle transition temperature of Cr_2AlC locates in the range of 700 to 800 °C. Accordingly, we select two temperatures of room temperature and 800 °C to study the effect of strain rate on the compressive behavior of Cr_2AlC.

The dependence of compressive strength on testing temperature is shown in Fig. 2b. It can be found that the compressive strength of Cr_2AlC specimen decreases continuously from 997 ± 29 MPa at room temperature to 749 ± 21 MPa at 800 °C and then drops significantly to

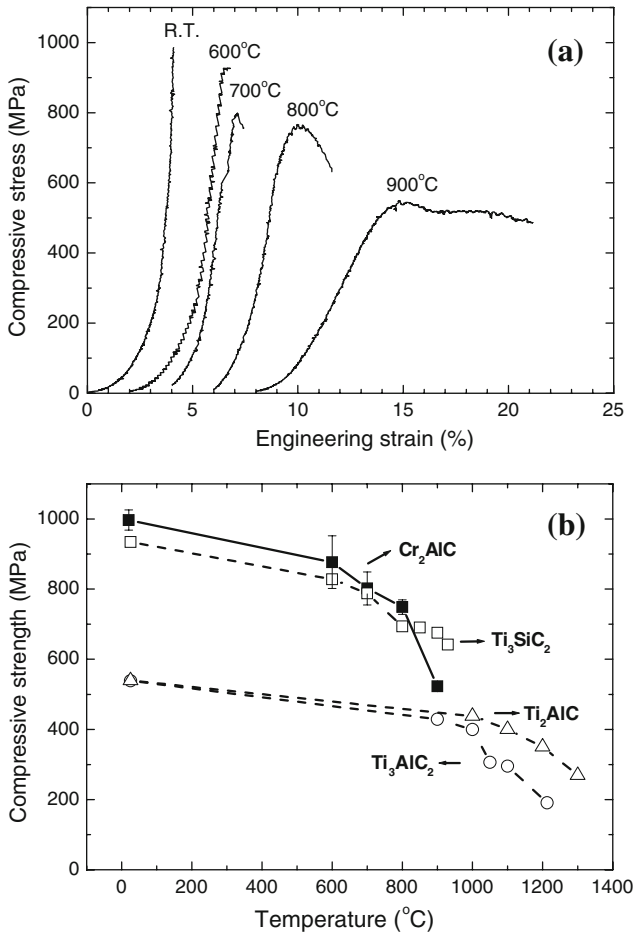

Fig. 2 **a** The relationship between compressive stress and engineering strain. **b** The dependence of compressive strength of Cr_2AlC specimens on the testing temperature. For comparison, the compressive strengths of Ti_3SiC_2, Ti_3AlC_2, and Ti_2AlC at different temperatures are also illustrated

523 ± 7 MPa at 900 °C, indicating that the compressive strength in the ductile mode is much more sensitive to temperature than that in the brittle regime. For comparison, the compressive strengths of Ti_3SiC_2 [22], Ti_3AlC_2 [23], and Ti_2AlC [24] at different temperatures are also plotted in Fig. 2b. It can be found that the compressive strengths of Cr_2AlC are not only higher than those of Ti_3AlC_2 and Ti_2AlC, but also slightly higher than those of Ti_3SiC_2 at temperatures below 800 °C. However, it becomes lower than that of Ti_3SiC_2 at the testing temperature of 900 °C, although it is still higher than that of Ti_3AlC_2 and Ti_2AlC. The high compressive strength of Cr_2AlC can be associated with the refined microstructure.

Figure 3a shows the stress–strain curves of Cr_2AlC specimens tested at room temperature at different strain rates. Despite the scatter in maximum compressive stresses recorded at different strain rates, these stress–strain curves of specimens tested at either higher strain rates or lower strain rates are similar to that of specimen tested at a strain rate of 5.6×10^{-4} s^{-1}, which is used as a standard strain rate for testing at different temperatures. This result indicates that the brittle deformation mode does not change in the strain rate range of 5.6×10^{-5} to 5.6×10^{-3} s^{-1} when tested at room temperature.

The stress–strain curves of Cr_2AlC specimens tested at 800 °C at different strain rates are shown in Fig. 3b. It is evident that the stress–strain curve varies from an elastic way to a plastic one as the strain rate decreases, and the plastic deformation region becomes more broadened as strain rate is below 5.6×10^{-4} s^{-1}, illustrating that the deformation mode changes from a ductile mode to a brittle mode when the strain rate is above 5.6×10^{-4} s^{-1}. Note that the specimens tested at 800 °C at low strain rates, such as 1.4×10^{-4} and 5.6×10^{-5} s^{-1}, do not break but display a spindle-like shape, similar to the specimen tested at 900 °C at a strain rate of 5.6×10^{-4} s^{-1}, revealing that high temperature and low strain rate have similar effect on the plastic deformation of Cr_2AlC.

The dependences of compressive strength of Cr_2AlC specimens on the strain rate at room temperature and at 800 °C are shown in Fig. 3c, in which it can be found that the compressive strength increases gradually with the increase in strain rate at room temperature, while it is less dependent on strain rate when tested at 800 °C.

Microstructural examination on the deformed and fracture surface

At certain strain rate (5.6×10^{-4} s^{-1}), the deformed and the fracture surfaces of the select but typical samples tested at room temperature and 800 °C are shown in Fig. 4a–d. When tested at room temperature, one main crack propagates through the specimen and makes about a 45° angle

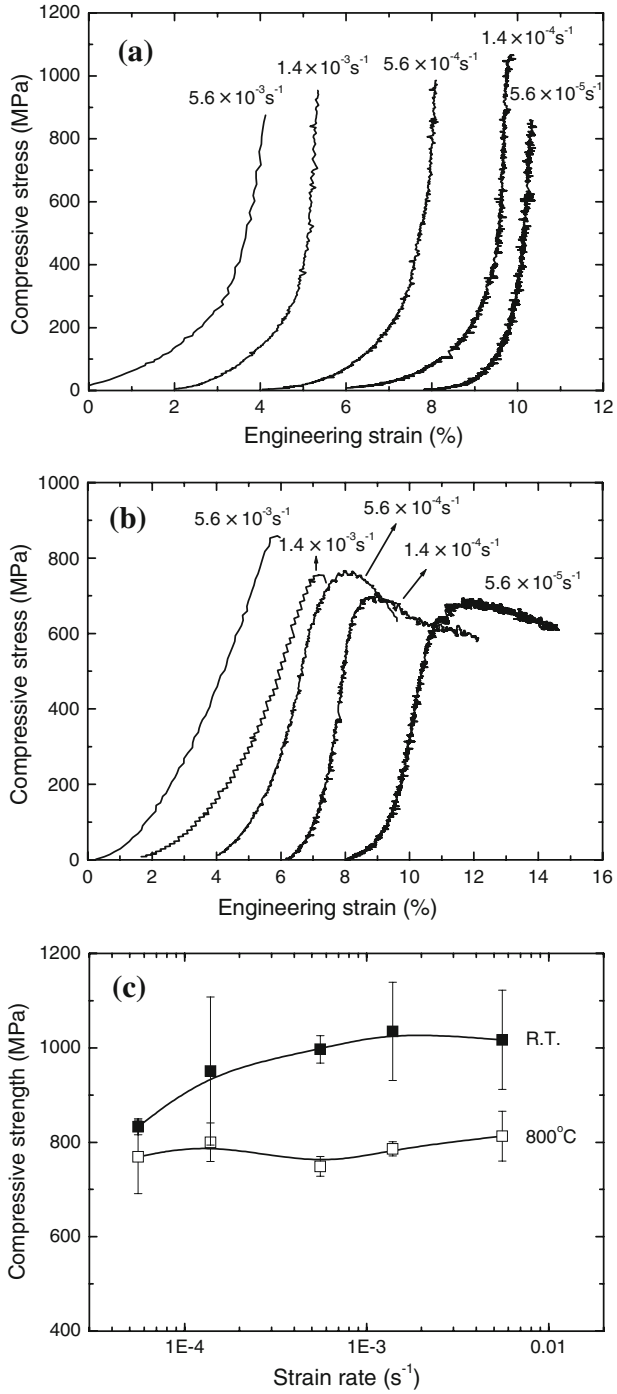

Fig. 3 The stress–strain curves of Cr_2AlC specimens tested at a different strain rate **a** at room temperature and **b** at 800 °C. **c** The dependences of strength on strain rate of Cr_2AlC specimens at room temperature and 800 °C

with the load direction (indicated as white arrow) (Fig. 4a). In contrast, when tested at 800 °C, a large number of cracks appear and most of them are aligned on the load direction (Fig. 4b). In addition, the fracture surfaces of the samples tested at all the testing temperatures are characterized predominantly by intergranular cracking, as represented by Fig. 4c (room temperature) and Fig. 4d (800 °C). Grain boundary decohesion is observed after compression at high temperature (Fig. 4e). Furthermore, delamination within grains on the fracture surface (Fig. 4f) can be found frequently in the specimens tested at 800 °C.

The microstructural images of specimens tested at room temperature at other strain rates are similar to those tested at 5.6×10^{-4} s^{-1} (Fig. 4a, c), and hence they are not shown. Figure 5 shows the deformed surface and the fracture surface of the sample tested at 800 °C at a high strain rate of 5.6×10^{-3} s^{-1}, in which the deformed region is confined in the vicinity of cracking area (Fig. 5a) and intergranular cracking characteristic, similar to the specimen tested at the same temperature at a strain rate of 5.6×10^{-4} s^{-1} (Fig. 4d), is also shown (Fig. 5b). Moreover, the kink band within grain is usually observed on the fracture surface, as shown in Fig. 5c.

Effect of temperature and strain rate on compressive properties

The difficult motion of dislocations at low temperatures and the lack of five independent slip systems are responsible for the absence of macro-plasticity in Cr_2AlC at a temperature below 700 °C, i.e., fracture in a brittle mode. By increasing the testing temperature, the motion of dislocations that is believed to be operative only at the basal plane [22–24] becomes readier and they will pile-up against the grain boundaries. The pile-ups would produce microcracks in various ways [25], such as grain buckling, kink band formation, etc. On the other hand, the cohesion strength of grain boundary decreases and the propagation of microcracks along grain boundaries becomes effective with increasing temperature. Furthermore, the microcracks will propagate with increasing applied stress during loading, leading to the grain boundary decohesion (Fig. 4e). It should be pointed out that the small amount of Al_2O_3 phases mostly distributed at grain boundary could also affect the mechanical strengths in two aspects: introducing tensile thermal stress in the Cr_2AlC matrix and weakening the grain boundary.

Note that a creep deformation, dislocation activity or diffusion-controlled creep, should be considered when the compressive tests were carried out at high temperatures. It is known that the diffusion-controlled creep needs to maintain the cohesion between deformed grains for the transport of material either along the grain boundary or throng the lattices of grains. However, based on the microstructural examination, it can be found that there are no obvious plastically deformed grains appeared but mostly consisting of intergranular cracking (Fig. 4b, e) and delamination (Fig. 4f) within grains. Therefore, it is reasonable to believe that the dominant high-temperature deformation mechanism in Cr_2AlC is related to the dislocation activities.

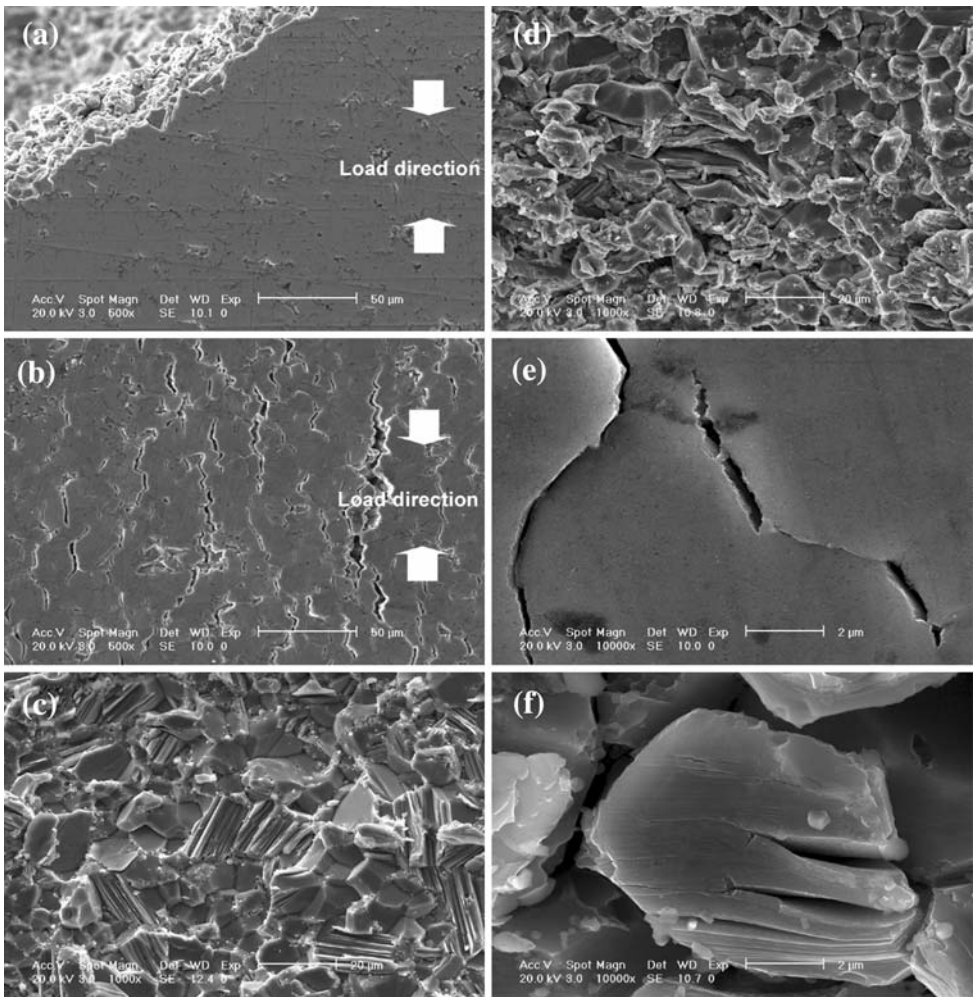

Fig. 4 The deformed surface of Cr_2AlC specimens tested **a** at room temperature and **b** 800 °C. The fracture surface of the sample tested **c** at room temperature and **d** 800 °C. **e** Typical grain-boundary decohesion and **f** delamination within grain in the Cr_2AlC specimens tested at 800 °C. All tests at a strain rate of 5.6×10^{-4} s^{-1}

At room temperature, the deformation mode is not sensitive to strain rate because of the difficult motion of dislocation. On the other hand, when tested at 800 °C, the deformation behavior depends on strain rate. This is contributed from more dislocations in the system activated at this elevated temperature. The brittle failure at a strain rate higher than 1.4×10^{-3} s^{-1} is attributed to insufficient time for the motion of activated dislocations to form microcracks and hence macro-structural plastic deformation.

Generally, the motion of dislocation is not only a thermally activated process, but also a stress-assisted process. Johnston and Gilman [26] reported that strain rate ($\dot{\varepsilon}$) is related to the dislocation velocity (v), which is in turn related to the shear stress for dislocation motion (τ) [27] according to the following equations:

$$\dot{\varepsilon} = \mathbf{b}nv, \tag{1}$$

$$v = \left(\frac{\tau}{\tau_0}\right)^P \tag{2}$$

where **b** is the Burgers vector, n the number of dislocation per unit area, τ_0 and P are experimentally determined material constants. Accordingly, the shear stress required for dislocation motion increases with the increasing strain rate. Therefore the compressive strength of Cr_2AlC increases with the increase in strain rate at room temperature, although the tendency is not so obvious at 800 °C (Fig. 3c). The mechanism for the less strain rate sensitivity at 800 °C than at room temperature needs further exploration, but it is likely related to the microstructural deformations, such as microcracks, delamination, and kink band.

Conclusion

The compressive strength of Cr_2AlC decreases continuously from 997 ± 29 MPa at room temperature down to 523 ± 7 MPa at 900 °C and this strength decreasing tendency is more obvious as the testing temperature is higher than 800 °C. Cr_2AlC compound fails in a brittle mode up to 700 °C and a ductile mode at and above 800 °C. At room temperature, the brittle deformation mode does not change

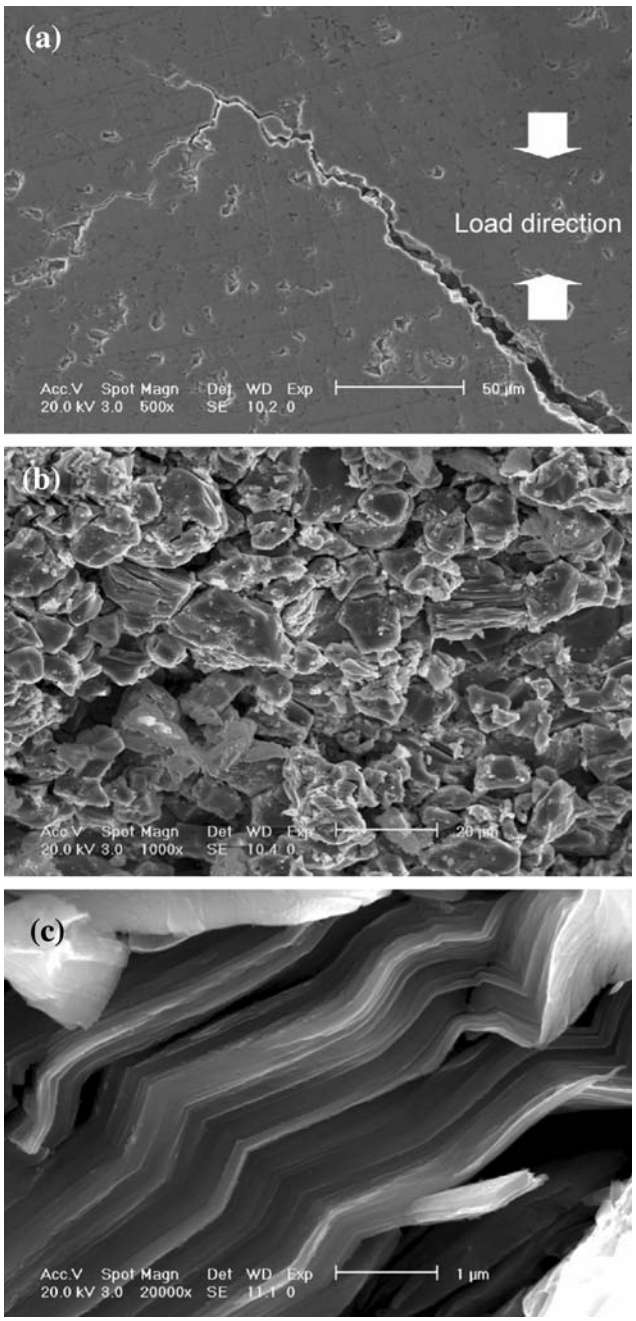

Fig. 5 **a** The deformed surface morphology and **b** the fracture surface of the Cr_2AlC specimen tested at 800 °C at a strain rate of 5.6×10^{-3} s^{-1}. **c** Typical kink band within grain on the fracture surface

in the tested strain rate range. At 800 °C, however, the deformation mode changes from a ductile mode to a brittle mode when the strain rate is above 5.6×10^{-4} s^{-1}. The compressive strength is almost independent of the strain rate especially when tested at 800 °C. The plastic deformation mechanism of Cr_2AlC can be explained by the dislocation-related activities, such as microcracks and decohesion of grain boundary and delamination and kink band within grains.

References

1. Barsoum MW (2000) Prog Solid State Chem 28:201
2. Barsoum MW, El-Raghy T (1996) J Am Ceram Soc 79:1953
3. Tzenov N, Barsoum MW (2000) J Am Ceram Soc 83:825
4. Salama I, El-Raghy T, Barsoum MW (2002) J Alloys Compd 347:271
5. Jeitschko W, Nowotny H, Benesovsky F (1963) Monatsh Chem 94:672
6. Schuster JC, Nowotny H, Vaccaro C (1980) J Solid State Chem 32:213
7. Schneider JM, Sun ZM, Mertens R, Uestel F, Ahuja R (2004) Solid State Commun 130:445
8. Schneider JM, Sigumonrong DP, Music D, Walter C, Emmerlich J, Iskandar R (2007) Scr Mater 57:1137
9. Walter C, Sigumonrong DP, El-Raghy T, Schneider JM (2006) Thin Solid Films 515:389
10. Walter C, Martines C, El-Raghy T, Schneider JM (2005) Steel Res Int 76:225
11. Lin ZJ, Zhou YC, Li MS, Wang JY (2005) Z Metallkd 96:291
12. Lin ZJ, Zhuo MJ, Zhou YC, Li MS, Wang JY (2006) J Appl Phys 99:076109
13. Lin ZJ, Li MS, Wang JY, Zhou YC (2007) Acta Mater 55:6182
14. Sun ZM, Ahuja R, Li S, Schneider JM (2003) Appl Phys Lett 83:899
15. Sun ZM, Li S, Ahuja R, Schneider JM (2004) Solid State Commun 129:589
16. Wang JY, Zhou YC (2004) Phys Rev B 69:244111-1
17. Wang JY, Zhou YC, Lin ZJ, Meng FL, Li F (2005) Appl Phys Lett 86:101902-1
18. Lofland SE, Hettinger JD, Harrell K, Finkel P, Gupta S, Barsoum MW, Hug G (2004) Appl Phys Lett 84:508
19. Tian WB, Wang PL, Zhang GJ, Kan YM, Li YX, Yan DS (2006) Scr Mater 54:841
20. Tian WB, Wang PL, Kan YM, Zhang GJ (2008) J Mater Sci 43:2785. doi:10.1007/s10853-008-2516-2
21. Tian WB, Wang PL, Zhang GJ, Kan YM, Li YX (2007) J Am Ceram Soc 90:1663
22. Radovic M, Barsoum MW, El-Raghy T, Wiederhorn SM, Luecke WE (2002) Acta Mater 50:1297
23. Barsoum MW, Zhen T, Kalidindi SR, Radovic M, Murugaiah A (2003) Nature Mater 2:107
24. Zhen T, Barsoum MW, Kalidindi SR (2005) Acta Mater 53:4163
25. Sun ZM, Zhang ZF, Hashimoto H, Abe T (2002) Mater Trans 43:432
26. Johnston WG, Gilman JJ (1959) J Appl Phys 30:129
27. Courtney TH (1990) Mechanical behavior of materials. McGraw-Hill Publishing Company, New York